Laser and Particle Beams (2005), *23*, 101–106. Printed in the USA.

DOI: 10.1017/S0263034605050172

Raman laser amplification in preformed and ionizing plasmas

D.S. CLARK[1] AND N.J. FISCH[2]

[1]Lawrence Livermore National Laboratory, Livermore, CA
[2]Princeton Plasma Physics Laboratory, Princeton, NJ

(RECEIVED 1 October 2004; ACCEPTED 2 November 2004)

Abstract

The recently proposed backward Raman laser amplification scheme utilizes the stimulated Raman backscattering in plasma of a long pumping laser pulse to amplify a short, and frequency downshifted seed pulse. The output intensity for this scheme is limited by the development of forward Raman scattering (FRS) or modulational instabilities of the highly amplified seed. Theoretically, focused output intensities as high as 10^{25} W/cm^2, and pulse lengths of less than 100 fs, could be accessible by this technique for 1 μm lasers—an improvement of 10^4–10^5 in focused intensity over current techniques. Simulations with the particle-in-cell (PIC) code Zohar are presented, which investigate the effects of FRS and modulational instabilities, and of Langmuir wave breaking on the output intensity for Raman amplification. Using the intense seed pulse to photoionize the plasma simultaneous with its amplification (and hence avoid plasmas-based instabilities of the pump) is also investigated by PIC simulations. It is shown that both approaches can access focused intensities in the 10^{25} W/cm^2 range.

Keywords: Langmuir wave-breaking; Laser ionization; Laser-plasma interaction; Raman laser amplification; Raman scattering

1. INTRODUCTION

The maximum output intensity achievable by the current chirp pulse amplification (CPA) technique for generating ultra-intense, ultra-short laser pulses is determined by the damage thresholds for final compressor gratings. To overcome this limit, the backward Raman amplification scheme has been proposed, in which plasma is used as the laser amplifying medium (Malkin *et al.*, 1999). In this scheme, a long pumping laser pulse collides with a short seed pulse downshifted in frequency from the pump by the plasma frequency in a preformed plasma slab. The seed pulse serves to stimulate the Raman backscatter of the pump into the seed with the result that, in the nonlinear regime, a characteristic π-pulse forms from the seed which both amplifies and compresses linearly with time. Theoretically, unfocused intensities of 10^{17} W/cm^2 in $\sim$50 fs pulses are accessible by this technique for 1 μm radiation. By focusing such pulses to near the diffraction limit, intensities of 10^{25} W/cm^2 become conceivable—a value 10^4 to 10^5 times greater than achievable by current CPA techniques.

Analogous to the nonlinear distortions and thermal degradations which limit output intensities for schemes based on solid material amplifiers or gratings (such as CPA), Raman amplification is limited (at much higher intensities) by instabilities which can arise from the interaction of the intense light pulses with the plasma. That is, energy may be transferred from the pump to the seed and the seed pulse amplified only for as long as the growth time of the fastest growing instability. After that point, the plasma must be terminated, and the amplified seed directed to its target before it is broken apart by the developing instability. For the Raman amplification regime, forward Raman scattering (FRS) (Antonsen & Mora, 1992) and modulational (Litvak, 1970; Max *et al.*, 1974) instabilities of the ultra-intense amplifying seed are the most likely saturation mechanisms. The growth times for these instabilities, and hence the amount of amplification of the seed, may be maximized by minimizing the background plasma density. In turn, the minimum allowable density for Raman amplification is determined by the threshold for Langmuir wave-breaking. Since the exchange of energy between the pump and seed in Raman scattering is mediated by a Langmuir wave, whose amplitude is determined by the strength of the pump, densities below the breaking threshold would disrupt the Langmuir wave, and degrade the energy transfer from the pump to the seed. Optimal performance of a Raman amplifier is then attained at the threshold for wave-breaking, with a plasma whose length is on the order of the minimum of the growth

Address correspondence and reprint requests to: D.S. Clark, Lawrence Livermore National Laboratory, P.O. Box 808, L-312, Livermore, CA 94551. E-mail: Clark90@llnl.gov

lengths of the FRS or modulational instabilities of the seed. Coincidentally, at the wave-breaking threshold, these growth lengths are approximately equal. In principle, the amplified seed pulse is also unstable to backward Raman scattering (BRS). Given that the seed pulse is compressing to ~50 fs pulse widths, any backscattered signal is, however, rapidly convected out of the pulse, and the growth of this instability should be very limited.

An interesting variation on the basic scheme of backward Raman amplification is the idea of ionizing Raman amplification (Malkin & Fisch, 2001). In the ionizing Raman amplification scheme, in place of a preformed (that is, ionized) plasma, a neutral precursor gas is used. Pump intensities below the photoionization threshold for that gas are then employed with a relatively more intense seed pulse, which acts to photoionize the gas as the seed is being amplified. Behind the ionization front formed at the leading edge of the seed pulse, Raman backscattering of the pump into the amplifying seed pulse occurs as in the preformed plasma case. Since the low intensity pump propagates only through the precursor gas, this scheme has the advantage of avoiding any possible spontaneous Raman backscatter of the pump prior to its intended interaction with the seed, an effect which could degrade or entirely disrupt the amplification process (Clark & Fisch, 2003). The preparation of the amplifying medium (in this case, a gas of specified uniform density) may also be far simpler than preparing plasma of the appropriate density, temperature, and uniformity needed for amplification in the conventional scheme. Finally, the added benefit of suppressing the formation of nonlinear precursors to the amplifying seed, which could also interrupt amplification, has also been shown in the presence of ionization (Clark & Fisch, 2002). Like the preformed plasma case, FRS and modulational instabilities of the intense seed pulse are again the leading saturation mechanisms likely to limit the final output intensity.

For both of these amplification schemes, previous investigations have largely used a cold plasma, 3-wave description of the resonant Raman interaction. While affording fast compute times, this numerical model does not inherently include the physics of wave-breaking, or the FRS or modulational instabilities critical in assessing the prospects of Raman amplification. By contrast, the fully kinetic model of the plasma represented by a PIC code naturally includes all of these physical processes and with great fidelity. In this paper, results from simulations run with the PIC code Zohar (Langdon & Lasinski, 1976) are presented, which investigate the effects of wave breaking and the saturation mechanisms in Raman amplification. Amplifications in both preformed and ionizing plasmas are considered.

2. EFFECT OF LANGMUIR WAVE-BREAKING

As shown by Malkin *et al*. (1999), specifying a certain pump intensity and wavelength specifies the length of the amplifier (approximately one growth length of the FRS or modulational instabilities) and the optimal plasma density for amplification (the density at which the driven Langmuir wave should just break). For linear polarization, these parameters are given by $L_{\mathrm{amp}} \sim c/\omega_1 a_1^2$ and $n_e = 4 n_c a_1^{4/3}$. Here, $a_1 = |e|\langle A_1\rangle/m_e c^2$ is the normalized amplitude for the pump laser, n_e is the electron number density, and n_c the critical density at the pump frequency. Analogously, $a_2 = |e|\langle A_2\rangle/m_e c^2$ and $a_3 = |e|\langle E_3\rangle/m_e c(\omega\omega_{pe})^{1/2}$ are the normalized amplitudes of the seed pulse and the resonant Langmuir wave. Below, ω_1 and ω_2 denoted the pump and seed laser frequencies, respectively, which are mismatched by the Langmuir wave frequency $\omega_{pe} = \omega_1 - \omega_2$ (neglecting thermal effects). In the following, only linearly polarized pump and seed lasers are considered, though the results for circularly polarized lasers would be similar.

These density and length scalings, however, are derived within the approximation of a cold plasma. Given that the pump beam in a Raman amplifier can be expected to heat the plasma to ~100 eV by the time the seed pulse is injected into the plasma, and also based on considerations of the stability of the pump beam to backscatter from thermal plasma noise (Clark & Fisch, 2003), $T_e = 200$ eV constitutes a more representative plasma temperature. For this temperature, some modification of the wave-breaking threshold from the cold plasma value, and hence of the density which optimizes the output seed pulse amplitude, can be expected. To assess this modification, a series of comparable PIC simulations with fixed temperatures of $T_e = 200$ eV and increasing plasma densities were run.

Choosing $a_1 = 0.015$, the threshold density for breaking of the backscatter-driven Langmuir wave in a cold plasma is $n_e \sim 0.015 n_c$. Figure 1 shows the results of a Zohar simulation of Raman amplification at this density and pump intensity. A long, pumping pulse (shown in blue) is first propagated

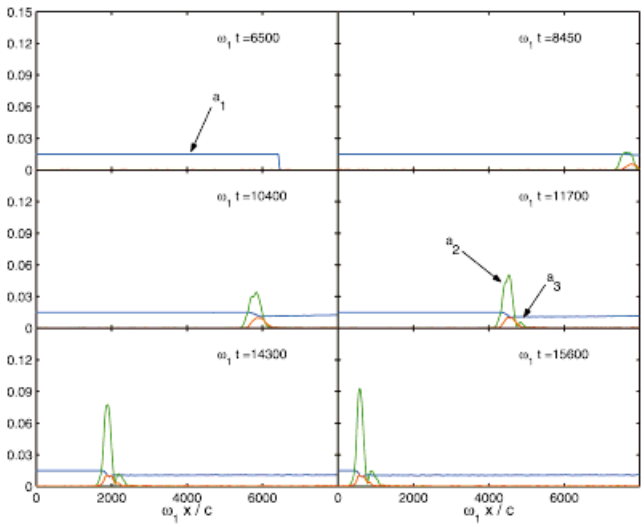

Fig. 1. Zohar simulation of Raman amplification at the cold plasma wave-breaking limit with $a_1 = a_2(t=0) = 0.015$, $n_e = 0.015 n_c$, $T_e = 200$ eV, and linear polarization.

across the plasma from the left and encounters the short seed pulse (shown in green) injected from the right. The interaction of the pump and seed generates a resonant Langmuir wave (shown in red), which backscatters the pump and so amplifies the seed. In contrast to the canonical amplification case, where the Langmuir wave persists in the plasma behind the seed pulse, here the Langmuir wave is seen to break in the neighborhood of the maximum of the seed pulse and allow only $\sim 30\%$ depletion of the pump.

The rapid breaking of the Langmuir wave and relatively low depletion of the pump in this simulation is evidence of the effect of the finite plasma temperature. Using the approximation of a "water bag" model for the electron distribution function, Coffey (1971) showed that thermal effects reduce the electric field at which wave-breaking can be expected by a factor of $(1 + 2\beta^{1/2} - 8\beta^{1/4}/3 - \beta/3)^{1/2}$ from the cold plasma value (Dawson, 1959). Here $\beta = 3(\mathrm{v_{te}}/\mathrm{v_{phase}})^2$. For the $T_e = 200$ eV initialized in the simulation, accounting for thermal effects by this "water bag" model raises the breaking threshold to $n_e \approx 0.05 n_c$, a factor of three greater than the cold plasma threshold.

Increasing the plasma density incrementally to $n_e = 0.025 n_c$ accomplishes greater depletion of the pump as shown in Figure 2. Similar to the initial results of Malkin *et al*. (1999), close to the wave-breaking threshold, a single spike forms for the amplifying pulse. Still greater depletion of the pump can be achieved by increasing the plasma density further, as shown in the simulation results in Figure 3 with $n_e = 0.035 n_c$. However, the extra energy extracted from the pump appears to result only in the formation of the secondary oscillations of a partial π-pulse, but does not increase the peak amplification of the leading spike. Breaking of the Langmuir wave is still evident (as can be verified from an x-p_x electron phase space plot) but is not as abrupt as in the lower density cases.

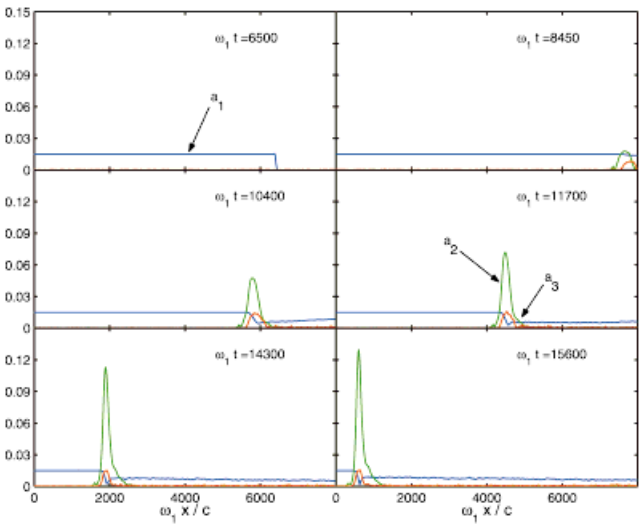

Fig. 2. Zohar simulation of Raman amplification above the cold plasma wave-breaking limit. The simulation parameters are the same as in Figure 1 but with $n_e = 0.025 n_c$.

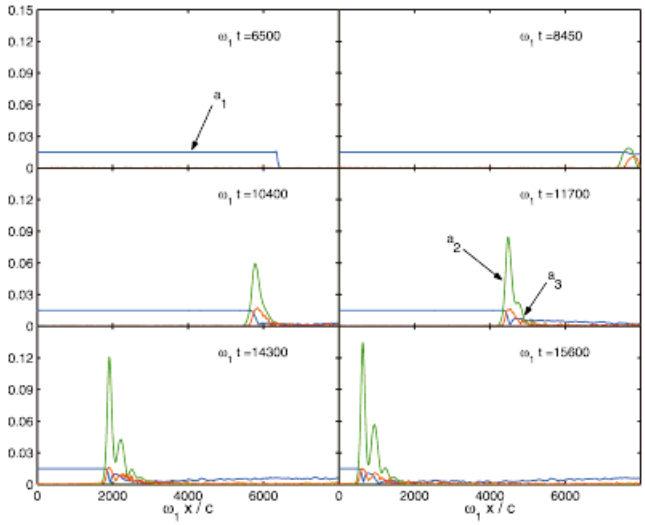

Fig. 3. Zohar simulation of Raman amplification above the cold plasma wave-breaking limit. The simulation parameters are the same as in Figure 1 but with $n_e = 0.035 n_c$.

In contrast to the expectations for a cold plasma, Figures 2 and 3 indicate that, for finite temperatures, optimal amplification occurs for a plasma density intermediate between the cold plasma breaking threshold ($n_e = 0.015 n_c$) and the threshold given by the formula of Coffey (1971) ($n_e = 0.05 n_c$). For these parameters, $n_e = 0.025 n_c$ yields the single optimally amplified spike, while below and above this density less amplification or amplification of only the tail of the pulse results. Since increasing n_e to greater than $0.025 n_c$ does not result in greater amplification of the leading spike, and can be expected to accelerate the onset of the saturating instabilities, ultimately less total amplification should be expected for $n_e > 0.025 n_c$.

3. SATURATION OF AMPLIFICATION

Saturation of Raman amplification may be studied simply by increasing the length of the computational domain in the simulations above. Figure 4 shows the result of repeating the simulation of Figure 2 with the simulation size increased by a factor of four. Between $\omega_1\, t = 57{,}200$ and $\omega_1\, t = 62{,}400$, the amplification effect has clearly been saturated and the seed pulse has begun to broaden and break apart. The result of zooming in on the seed pulse in the last two frames of Figure 4 is shown in Figure 5. A strong spike has formed at the tail of the seed pulse which, though in principle is an amplification of the seed, indicates the disruption of the π-pulse, and the termination of the contracting and amplifying self-similar solution. Just prior to saturating, the single amplified spike has reached an amplitude of $a_2 \sim 0.25$ or intensity of 3.4×10^{17} W/cm^2 for $\lambda = 0.532$ μm in quite close agreement with the value expected from Malkin *et al*. (1999).

The nonlinear mechanism responsible for this saturation can be identified from the k_x spectrum for this simulation as

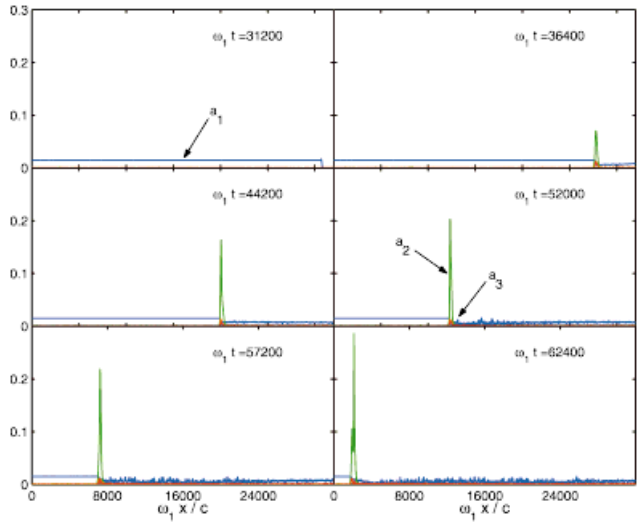

Fig. 4. Zohar simulation showing saturation of Raman amplification near the wave-breaking limit: $n_e = 0.025 n_c$. The simulation parameters are the same as in Figure 2 but with the simulation domain lengthened by a factor of four.

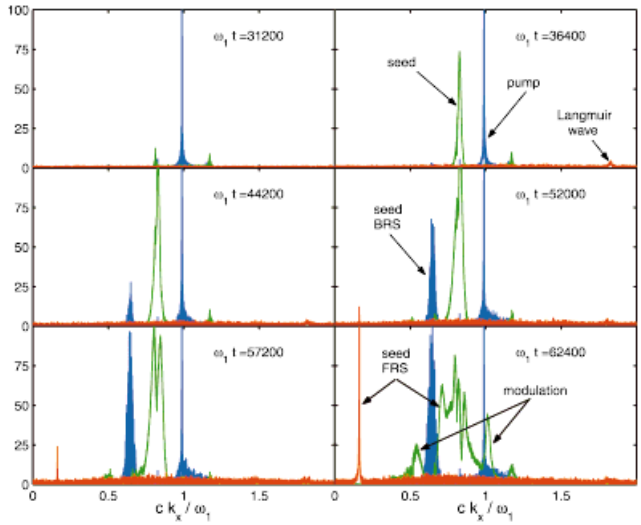

Fig. 6. k_x spectrum from the simulation of Figure 4. The right-propagating power spectrum is shown in blue, the left-propagating spectrum in green, and the spectrum of the longitudinal electric field is shown in red.

shown in Figure 6. Here, the power spectrum of right-propagating energy (that is, in the direction of the pump) is shown in blue, the spectrum of left-propagating energy (in the direction of the seed) is shown in green, and the spectrum of the longitudinal electric field (the Langmuir wave) is shown in red. Initially, the seed pulse is seen to amplify as well as broaden in k_x corresponding to its spatial narrowing with amplification. The resonantly driven Langmuir wave corresponds to the small signal at $ck_x/\omega_1 \approx 1.84$. Beginning from $\omega_1\, t = 57{,}200$, the substantial Langmuir oscillation at $k_x \approx \omega_{pe}/c \approx 0.16\ \omega_1/c$ accompanied by the down-shifted side-band of the seed pulse at $k_x \approx 0.68\ \omega_1/c$ is indicative of Raman forward scattering of the seed. These signals become very prominent for $\omega_1\ t = 62{,}400$ along with a general broadening of the seed spectrum. Also appearing at this time are side-bands at $k_x \approx k_2\ (1 \pm a_2) \approx k_2\ (1 \pm 0.25)$, the wave numbers characteristic of the modulational instability. Remarkably, a substantial degree of Raman backscatter of the seed pulse is seen from $\omega_1\, t = 44{,}200$ onward in the form of the right-propagating signal down-shifted from the seed pulse signal by ω_{pe}/c.

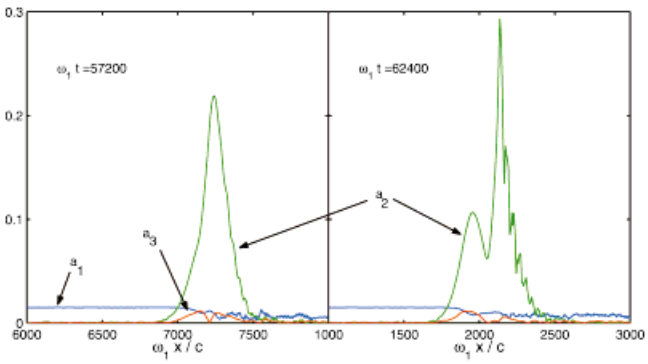

Fig. 5. Result of zooming in on the seed pulses from the last two frames of Figure 4. The π-pulse shape breaks apart indicating saturation of amplification.

4. AMPLIFICATION IN IONIZING PLASMAS

As in the case of amplification in preformed plasmas, PIC simulations provide a valuable tool both for verifying the basic amplification effect and for studying the saturation of amplification in ionizing plasmas. Figure 7 shows snapshots from a simulation of ionizing amplification using an initially trapezoidal-shaped seed pulse of peak amplitude $a_2 = 0.007$, that is, just above the threshold for rapid photoionization. The working gas for this case is hydrogen with $n_n = 0.001 n_c$, the pump enters the simulations box from the left with an amplitude of $a_1 = 0.0015$ (corresponding to $I_{\text{pump}} = 10^{13}$ W/cm^2) and $\lambda = 0.532\ \mu$m. Here the laser envelopes are plotted in the frame following the seed pulse such that the neutral gas effectively flows in from the left. The abrupt leading edge of the seed pulse for $\omega_1\, t > 0$ corresponds to the steep ionization front behind which the plasma is effectively fully ionized. Behind this ionization front, the Langmuir wave is seen to form and strongly backscatter the pump.

In comparison with the preformed plasma results shown in Figures 1 to 6, the seed pulse profile from Figure 7 displays pronounced modulations in amplitude on the order of 20%. The k_x spectrum for this simulation shown in Figure 8 suggests the origin of these modulations as being the strong blue-shifting of the seed pulse spectrum evident from $\omega_1\, t = 2.1 \times 10^5$ onward. This blue-shifting is well-known to result from the seed pulse's co-propagation with the ionization front (Rae & Burnett, 1992; Esarey *et al.*,

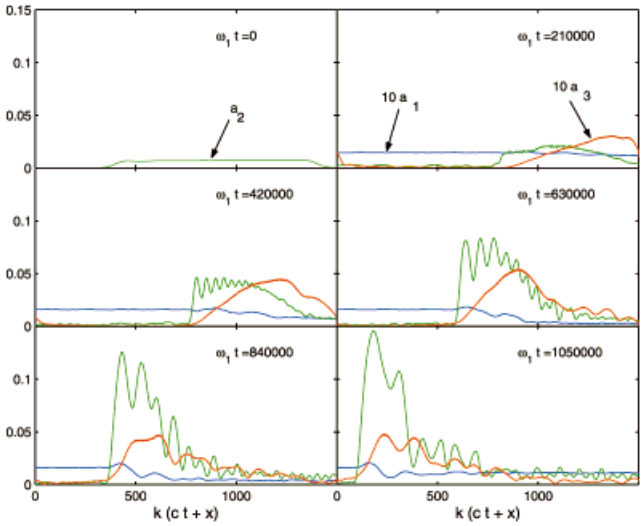

Fig. 7. Zohar simulation of Raman amplification in an ionizing hydrogen plasma with $a_1 = 0.0015$, $a_2(t = 0) = 0.007$, $n_n = 0.001 n_c$, $\lambda = 0.532$ μm, and linear polarization. The pump and seed envelopes are shown multiplied by 10 for clarity.

1991). Indeed, filtering the k_x spectrum of this blue component and replotting the result in physical space yields a smooth seed profile quite similar to those from Figure 5.

As evidenced by the limited pump depletion in the last frame of Figure 7, the amplification process has been saturated by $\omega_1 t = 1.0 \times 10^6$ with $a_2 = 0.15$. The characteristic forking of the leading spike of the seed pulse (as also seen in Fig. 5) is also evident at this time. Again, the k_x spectrum shows the signatures of FRS and modulational instabilities as the saturation mechanisms. A peak output intensity of

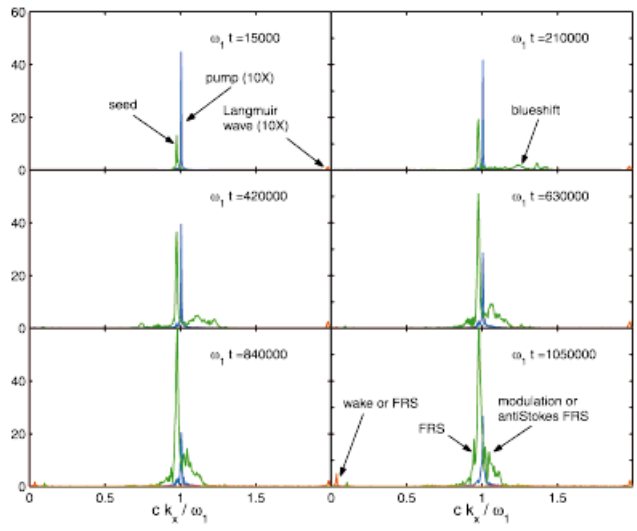

Fig. 8. k_x spectrum from the simulation of Figure 7. The right-propagating power spectrum is shown in blue, the left-propagating spectrum in green, and the spectrum of the longitudinal electric field is shown in red.

$I_{\text{out}} = 1.2 \times 10^{17}$ W/cm^2 is reached, verifying that comparable intensities can be reached via the ionizing amplification scheme as by amplification in preformed plasmas. Note that the much lower pump intensities required for ionizing amplification (so as not to exceed the ionization threshold of the precursor gas) entail much longer interaction lengths for the same output intensity in comparison with preformed plasmas. In this case, an amplification length of $\sim$7 cm is required as compared with the $\sim$5 mm for the simulation as shown in Figure 5. Given that the prepared interaction medium is merely a gas of the specified density, this longer length scale may not present any difficulty.

5. CONCLUSIONS

In summary, PIC simulations with the Zohar code were used to investigate the effects of wave breaking and saturation in Raman amplification. It was verified that operating as close as possible to the wave breaking limit achieves the strongest amplification of the seed: Once below the density threshold at which the Langmuir wave breaks before the first peak of the seed pulse, the degree of pump depletion and hence seed amplification declines rapidly with decreasing density. For densities above the breaking threshold, stronger depletion of the pump occurs but serves only to amplify the secondary oscillations of the π-pulse without amplifying the leading spike, while deleterious instabilities which limit the total amplification develop more rapidly and reduce the maximum achievable amplification. For the representative plasma temperature of $T_e = 200$ eV, it was found that a plasma density intermediate between the breaking threshold for a cold plasma and the threshold predicted by the theory of Coffey (1971) yielded the optimally amplified single spike. At the optimal plasma density, saturation of the amplification effect was observed at an intensity of $\sim 10^{17}$ W/cm^2 in the form of the amplified pulse breaking into two lobes and depletion of the pump ceasing.

For the case of ionizing amplification, PIC simulations demonstrated saturation of the amplification effect also to occur by FRS and modulational instabilities of the seed. Output intensities comparable to those for preformed plasmas ($\sim 10^{17}$ W/cm^2) were still attained but at the cost (due to the requirement of much lower pump intensities) of significantly longer interaction lengths. Modulation of the seed pulse profile was also found to occur due to blueshifting of the seed pulse spectrum in its co-propagation with the ionization front.

ACKNOWLEDGMENTS

The help of A.B. Langdon in preparing simulations with Zohar and on the general theory and method of PIC simulation is gratefully acknowledged. This work was supported by the U.S. Department of Energy Contract No. DE-AC02-76-CHO-3073 and the Defense Advanced Research Projects Agency (DARPA).

REFERENCES

Antonson, T.M. & More, P. (1992). Self-focusing and Raman scattering of laser pulses in tenuous plasmas. *Phys. Rev. Lett.* **69**, 2204.

Clark, D.S. & Fisch, N.J. (2002). Regime for a self-ionizing Raman laser amplifier. *Phys. Plasmas* **9**, 2772.

Clark, D.S. & Fisch, N.J. (2003). Operating regime for a backward Raman laser amplifier in preformed plasma. *Phys. Plasmas* **10**, 3363.

Coffey, T.P. (1971). Breaking of large amplitude plasma oscillations. *Phys. Fluids* **14**, 1402.

Dawson, J.N. (1959). Nonlinear electron oscillations in a cold plasma. *Phys. Rev.* **113**, 383.

Esarey, E., Joyce, G. & Sprangle, P. (1991). Frequency up-shifting of laser pulses by copropagating ionization fronts. *Phys. Rev. A* **44**, 3908.

Langdon, A.B. & Lasinski, B.F. (1976). *Electromagnetic and relativistic plasma simulation models*. In *Methods in Computational Physics* (Killeen, J., Alder, R., Fernbach, S. & Rotenberg, M., Eds.), pp. 327–266, New York: Academic Press.

Litvak, A.G. (1970). Finite-amplitude wave beams in a magnetoactive plasma. *Sov. Phys. JETP* **30**, 344.

Malkin, V.M., Shvets, G. & Fisch, N.J. (1999). Fast compression of laser beams to highly overcritical powers. *Phys. Rev. Lett.* **82**, 4448.

Malkin, V.M. & Fisch, N.J. (2001). Backward Raman amplification of ionizing laser pulses. *Phys. Plasmas* **8**, 4698.

Max, C., Arons, J. & Langdon, A.B. (1974). Self-modulation and self-focusing of electromagnetic waves in plasmas. *Phys. Rev. Lett.* **33**, 209.

Rae, S.C. & Burnett, K. (1992). Detailed simulations of plasma-induced spectral blueshifting. *Phys. Rev. A* **46**, 2077.